

Pseudoscalar and vector meson Production in NN Collisions *

K. NAKAYAMA^{a,b}

^aDepartment of Physics and Astronomy, University of Georgia, Athens, GA
30602, USA

^bInstitut für Kernphysik, Forschungszentrum-Jülich, D-52425, Jülich, Germany

(Received October 30, 2018)

Heavy meson production in nucleon-nucleon collisions is discussed within a meson exchange model of hadronic interactions, paying special attention to the basic dynamics that determine the behavior of the cross sections near the threshold energy. The $pp \rightarrow pp\phi$ reaction is discussed as an example of the production of vector mesons in NN collisions. For the pseudoscalar meson production, results for the η production in both the pp and pn collisions are presented.

* Invited lecture presented at the symposium on "Threshold Meson Production in pp and pd Interaction", June 2001, Cracow, Poland

1. Introduction

With the advent of particle accelerators in the few GeV energy region, heavy meson production in hadronic collisions has attracted increasing attention in the past few years. In particular, heavy meson production in nucleon-nucleon (NN) collisions is of special interest because it allows to investigate in a simple system the short range hadron dynamics for which, so far, we have a very limited knowledge. Due to the large momentum transfer between the initial and final states, these reactions necessarily probe the dynamics at short distances. In this context, apart from the intrinsic interest associated with the particular meson produced, the production of pseudoscalar and vector mesons can be used as a tool to probe the short distance dynamics systematically. Table 1 illustrates this point: it shows the momentum transfer and the corresponding distance probed by producing mesons of different masses at the respective threshold energy. At threshold, the momentum transfer is given by $q = (m_N m_M + m_M^2/4)^{1/2}$, where m_N and m_M denote the nucleon and meson mass, respectively. As one can see, the distance probed in these reactions ranges from $0.53fm$ for pion production to $0.18fm$ for ϕ meson production.

Table 1. Momentum transfer q and the corresponding distance r probed by the $NN \rightarrow NNM$ reaction at the threshold energy for different particles M produced.

particle	mass (MeV)	q (fm^{-1})	r (fm)
γ	0	0.0	∞
π	140	1.9	0.53
η	550	3.9	0.26
ρ, ω	780	4.8	0.21
η'	960	5.4	0.19
ϕ	1020	5.6	0.18

The theory of heavy meson production is still in its early stage of development. As we have seen above, heavy meson production reactions can probe quite short distances - down to less than $0.2fm$. These short distances correspond to the region of confinement where the relevant degrees of freedom are the constituent quarks and gluon flux tubes. Thus, the appropriate approach to describe these short range dynamics might be the constituent quark models rather than the hadronic models. However, such an approach still remain to be developed. On the other hand, the transition region from the hadronic to constituent quark degrees of freedom does not have a well-defined boundary and, consequently, it is of special interest to see how far down in distance one can “push” the hadronic models.

In principle, effective field theories can be used to describe near-threshold particle production processes in terms of hadronic degrees of freedom. However, although such an approach (Chiral Perturbation Theory) might be appropriate for describing the production of pions [1] in spite of the relatively large expansion parameter, $Q = \sqrt{m_\pi/m_N} \sim 1/3$, for the description of heavy meson production there is, *a priori*, no obviously preferred approach. The majority of existing calculations of heavy meson production in NN collisions are based on meson exchange models of strong interactions [2, 4, 3, 5, 6, 7, 9, 10, 11, 12] with a few exceptions [13]. The price one pays for insisting on such models is that their predictions become more and more sensitive to the short range part of the model, usually parametrized in terms of the form factors at the hadronic vertices involved. The success of such models should be measured in terms of their capability to correlate as many independent processes as possible in a consistent manner. We mention that although the approach used in Ref.[12] is based on meson exchange models, it differs from conventional meson exchange models in a number of aspects, such as the absence of the form factors at the hadronic vertices, etc.

2. Meson Exchange Models

As mentioned in the previous section, the majority of the existing calculations of meson production in NN collisions are based on conventional meson exchange models. Even within such models, the description of these reactions is not a simple task in principle, for the final state is a three-body state and, consequently, one needs to solve the three-body Faddeev equation. Of course, a complete three-body calculation of this reaction is at present not available [14]. How can one then start to describe these reactions? In order to gain some insight to this question, let us examine some of the features exhibited by the production cross sections near threshold. In reactions like NN bremsstrahlung, where a (massless) photon is produced, the measured cross section varies with the inverse of the photon energy ω_γ near threshold. This feature of the cross section is expressed by the so-called soft-photon theorem [15] which gives

$$\sigma = \frac{A}{\omega_\gamma} + B , \quad (1)$$

where A and B are constants containing only the on-shell information of the NN interaction (or, in other words, the asymptotic behavior of the NN wave function). This result is not surprising at all if we recall from Table 1 that, close to threshold, the photon production reaction in NN collisions probes only the asymptotic behavior of the NN wave function. Eq.(1) is,

therefore, regarded as a model-independent result and, as such, it should be reproduced by any model describing the NN bremsstrahlung reaction.

For production of heavy mesons, we do not have a model independent result like the low energy theorem for NN bremsstrahlung. However, as early as 1952, Watson [16] showed that in heavy particle production reactions in which strongly (attractively) interacting particles are present, the energy dependence of the cross sections should be dictated by the energy dependence of the interaction between those strongly interacting particles and the available phase space. In particular, for meson production in NN collisions, the energy dependence of the total cross section should be given by the energy dependence of the on-shell NN final state interaction (FSI), $T(p', p')$, plus the phase space

$$\begin{aligned} \sigma(E) &\propto \int d\rho(E, p') |T(p', p')|^2 \\ &\propto \int d\rho(E, p') \left(\frac{\sin(\delta(p'))}{p'} \right)^2, \end{aligned} \quad (2)$$

where the integration is over the available phase space, $\rho(E, p')$, with p' denoting the relative momentum of the two interacting nucleons in the final state. $\delta(p')$ denotes the corresponding NN phase shift. Watson's result is based on the observation that the massive particle production is a short range process and, as such, the primary production amplitude of such a particle should have a weak energy dependence. Note that the production cross section $\sigma(E)$ cannot be expressed in a model-independent way, for its absolute value depends on the short range part of the interaction. We shall elaborate more on Watson's result later. For the moment, we mention that all the recently measured meson production cross sections in NN collisions near threshold follow the energy dependence given by Eq.(2) with the exception of η meson production, where one sees a relatively small deviation at energies close to threshold. This deviation is commonly attributed to the ηN FSI.

The above consideration indicates that any model of heavy meson production reaction in NN collisions should have built in the feature given by Watson's result, Eq.(2). As we shall show in the following, this can be achieved within a Distorted Wave Born Approximation. Here we follow a diagrammatic approach to derive the total amplitude. We start by considering the meson-nucleon (MN) and NN interactions as the building blocks for constructing the total amplitude describing the $NN \rightarrow NNM$ reaction. We then consider all possible combinations of these building blocks in a topologically distinct way, with two nucleons in the initial state and two nucleons plus a meson in the final state. In this process of constructing

the total amplitude, care must be taken in order to avoid diagrams that lead to double counting. Specifically, these are the diagrams that lead to the mass and vertex renormalizations, since we choose to use the physical masses and coupling constants. The resulting amplitude constructed in this way is displayed in Fig. 1. The ellipsis indicates those diagrams that are

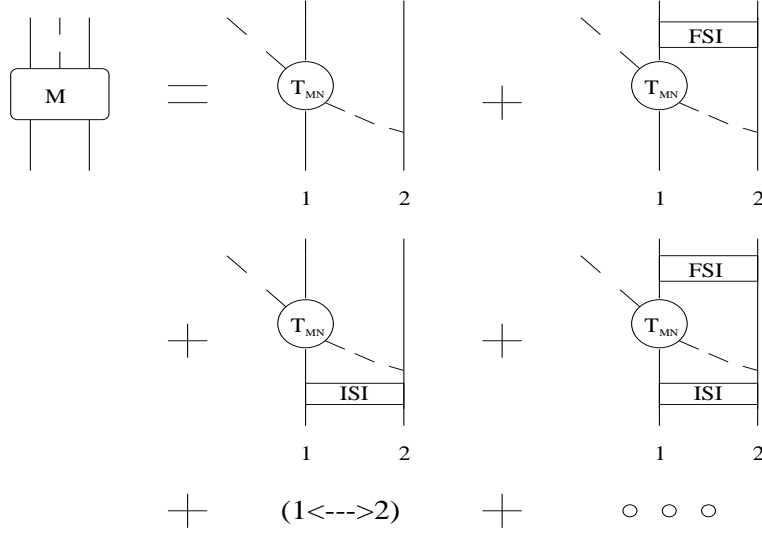


Fig. 1. Meson production amplitude obtained in a diagrammatic approach to the $NN \rightarrow NNM$ reaction considering the MN and NN T -matrices as the basic building blocks. T_{MN} stands for the MN T -matrix. FSI and ISI stand for the final and initial state NN T -matrices, respectively. The first diagram on the r.h.s. is referred to as the production current J which enters in other diagrams as can be noted.

more involved numerically (including, in particular, the MN FSI, which otherwise would be generated by solving the three-body Faddeev equation). So far there are very few attempts to account for them [6, 17]. Therefore, neglecting those diagrams, the total amplitude is given by the diagrams displayed explicitly in Fig. 1 and reads

$$M = (1 + T_f^{(-)\dagger} G_f^{(-)*}) J (1 + G_i^{(+)} T_i^{(+)}), \quad (3)$$

where $T_{(i,f)}$ denotes the NN T -matrix interaction in the initial(i)/final(f) state and, $G_{(i,f)}$, the corresponding two nucleon propagator. The superscript \pm in $T_{(i,f)}$ as well as in $G_{(i,f)}$ indicates the boundary condition ($-$) for incoming and $(+)$ for outgoing waves). The production current is denoted by J , which is nothing other than the MN T -matrix, T_{MN} , with

one of the meson legs attached to a nucleon (first diagram on the r.h.s. in Fig. 1). Eq.(3) is the basic formula on which the large majority of existing calculations are based.

We now wish to exhibit the essential features of the meson production reaction contained in Eq.(3). In particular, we would like to make close contact between the amplitude M and Watson's result given by Eq.(2). To this end, we use the relation

$$G_\alpha^{(\pm)} = \mathcal{P} \left(\frac{1}{E_\alpha - E(k)} \right) \mp i\pi\delta(E_\alpha - E(k)) , \quad (4)$$

where $\alpha = i, f$, to express M as

$$\begin{aligned} M &= \left\{ 1 - i\kappa_f T_f(p', p') [1 + i\frac{1}{ap'} \mathcal{P}_f(E, p')] \right\} J(E, p') \\ &\times \left\{ 1 - i\kappa_i T_i(p, p) [1 + i\frac{1}{ap} \mathcal{P}_i(E, p')] \right\} , \end{aligned} \quad (5)$$

where $T_i(p, p)$ denotes the on-shell NN T-matrix with the relative momentum p of the interacting two nucleons in the initial state i and $T_f(p', p')$ denotes the on-shell NN T-matrix with the relative momentum p' of the interacting two nucleons in the final state f . Here the superscript (+) of $T_{(i,f)}$ has been omitted. $\kappa_i \equiv \pi p \varepsilon(p)/2$ and $\kappa_f \equiv \pi p' \varepsilon(p')/2$ are the phase space densities of the two nucleons in the initial and final states, respectively. $\varepsilon(q) \equiv \sqrt{q^2 + m_N^2}$ and a is a constant (scattering length) introduced for convenience. Note that in the above equation, only those arguments of the quantities relevant to the discussion related to Watson's result are explicitly displayed. $E \equiv E_i$. The function \mathcal{P}_i is given by

$$\mathcal{P}_i(E, p') = \left(\frac{ap}{\kappa_i} \right) \mathcal{P} \int_0^\infty dk k^2 \frac{f_i(E, k)}{E_i - E(k)} , \quad (6a)$$

$$f_i(E, k) \equiv \frac{T_i(p, k)J(E, k)}{T_i(p, p)J(E, p')} = \frac{K_i(p, k)J(E, k)}{K_i(p, p)J(E, p')} . \quad (6b)$$

Similarly,

$$\mathcal{P}_f(E, p') = \left(\frac{ap'}{\kappa_f} \right) \mathcal{P} \int_0^\infty dk k^2 \frac{f_f(E, k)}{E_f - E(k)} , \quad (7a)$$

$$f_f(E, k) \equiv \frac{T_f(p', k)A(E, k)}{T_f(p', p')A(E, p')} = \frac{K_f(p', k)A(E, k)}{K_f(p', p')A(E, p')} , \quad (7b)$$

with $K_{(i,f)}$ denoting the NN K-matrix and $A \equiv (1 + G_i T_i)J$. The functions $\mathcal{P}_{(i,f)}(E, p')$ summarize all the off-shell effects of the NN interaction and

production current. As such, they are unmeasurable and model-dependent quantities. For production of heavy mesons near threshold, the off-shell NN interaction required in $\mathcal{P}_f(E, p')$ is at very low energy. In calculations based on conventional meson exchange models this function is very large and cannot be neglected. In contrast, the function $(1/ap)\mathcal{P}_i(E, p')$ is relatively small. This is because for heavy meson production the energy of the two nucleons in the initial state has to be large enough to produce the meson in the final state. For example, for η meson production, the incident energy of the beam nucleon corresponding to the threshold energy is about $1.25 GeV$. At such high energies, the on-shell NN interaction has a rather weak energy dependence. Note that the inverse scattering theory tells us that, for a local and energy-independent NN potential, the off-shell behavior of the NN amplitude is completely determined if one knows the corresponding on-shell amplitude in the entire energy domain. At least in the case of meson exchange models, the weak energy dependence of the on-shell NN interaction implies also a flat off-shell behavior and leads to a small value of $(1/ap)\mathcal{P}_i(E, p')$. Therefore, at least for the discussion of the essential features of the cross section near threshold, the function $(1/ap)\mathcal{P}_i(E, p')$ may be neglected.

Using then the relation between the on-shell T-matrix and the phase shift $\delta(q)$ and inelasticity $\eta(q)$

$$\kappa(q)T(q, q) = \frac{i}{2} \left(\eta(q)e^{2i\delta(q)} - 1 \right) , \quad (8)$$

Eq.(5) can be reduced to

$$M \cong \left\{ -e^{i\delta_f(p')} \left(\frac{\sin(\delta_f(p'))}{ap'} \right) [1 + \mathcal{P}_f(E, p')] \right\} J(E, p') \\ \times \left\{ \frac{1}{2} \left(\eta_i(p)e^{i2\delta_i(p)} + 1 \right) \right\} , \quad (9)$$

where the inelasticity in the final NN state is set to unity, $\eta_f(p') = 1$. The above equation is the desired result. It exhibits the essential features of the meson production reaction in NN collisions. First, it shows that the relevant energy dependence of the total amplitude near threshold is indeed determined by the strong energy dependence of the on-shell NN FSI, proportional to $\sin(\delta_f(p'))/ap'$. This, when combined with the phase space factor, determines the energy dependence of the cross section as given by Eq.(2). Note that for heavy meson production the production current $J(E, p')$, as well as $\mathcal{P}_f(E, p')$, should be weakly energy-dependent, for they summarize all the short range dynamics of the reaction. Thus, none of the terms in Eq.(9), apart from the on-shell NN FSI, should introduce any significant energy dependence near threshold; they just amount to a constant.

Therefore, the total cross section data near threshold determine just this constant. Second, the major effect of the NN initial state interaction (ISI) (the term in the last curly brackets) is to reduce the cross section by a factor of

$$\begin{aligned} \lambda &= \left| \frac{1}{2} \left(\eta_i(p) e^{i2\delta_i(p)} + 1 \right) \right|^2 \\ &= \eta_i(p) \cos^2(\delta_i(p)) + \frac{1}{4} [1 - \eta_i(p)]^2 \leq \frac{1}{4} [1 + \eta_i(p)]^2 . \end{aligned} \quad (10)$$

As mentioned before, the majority of the existing calculations of meson production in NN collisions are based on Eq.(3). The differences among them reside in how the production current J is modeled, as well as in the different treatments of both the NN FSI and ISI. Let's first concentrate on the NN interactions. It is clear that the description of meson production processes in NN collisions based on Eq.(3) requires the half-off-shell NN ISI and FSI. This has been exhibited explicitly in Eq.(5) through the functions $\mathcal{P}_{(i,f)}$ given by Eqs.(6,7). Although the on-shell NN interaction can be determined from the NN elastic scattering experiments, the off-shell behavior of it can only be provided by a given model of the NN interaction. For energies below pion threshold, there exist a number of accurate meson exchange models [18, 19, 20] which can provide the half-off-shell extension of the NN interaction. As previously noted, these so-called realistic NN interactions, based on meson exchange models, yield a rather large value for the function $\mathcal{P}_f(E, p')$ that, consequently, cannot be neglected. In this connection, for production of heavy mesons, the predicted total cross sections can easily differ by a factor of two or more due to the different off-shell behavior of these realistic NN FSIs. This indicates that a consistent treatment of the NN FSI and the production current J is required. Maintaining the consistency between the NN FSI and the production current, however, is not a trivial task. While in models where the underlying meson exchange structure is known this consistency can, in principle, be maintained, in the case of purely phenomenological models, such as the parametrized version of the Paris NN interaction [19], such a consistency is impossible to achieve - even in principle. In the excess energy region below $Q \cong 100 \text{ MeV}$ however, the introduced difference in the predicted total cross section due to off-shell differences of these realistic NN interactions is practically a constant. It should also be mentioned that the procedure of just evaluating J in the on-shell tree level approximation and simply multiplying it by the on-shell NN FSI, as has been done by many authors (see references quoted in [21]), is not acceptable for obtaining quantitative predictions. As it can be seen from Eq.(9), the strength of the amplitude M depends on the function $\mathcal{P}_f(E, p')$. Using just the on-shell T -matrix as the FSI instead of the full half-off-shell

T -matrix means setting the function $\mathcal{P}_f(E, p')$ to zero. Such a procedure simply lacks a consistent regularization scheme between the NN interaction and the production current J [21].

One of the major limitations in the current models of heavy meson productions in NN collisions is the lack of a reliable model for the NN ISI. As mentioned before, the energy of the two interacting nucleons in the initial state must be large enough to produce a meson. For example, for the η meson this means nucleon incident energies of at least 1.25 GeV . For heavier mesons, like η' and ϕ , the corresponding threshold incident energy is well above 2 GeV , where no reliable model exists to provide the half-off-shell NN T -matrix that is required in the evaluation of the function $\mathcal{P}_i(E, p')$ in Eq.(6). Note that, although this quantity is expected to be small and may be neglected for estimates of cross sections, for more quantitative predictions it should be taken into account. In particular, predictions of spin observables are expected to be sensitive to this function. The situation with the NN ISI is even worse in the case of heavy meson production in pn collisions. There, we lack even the on-shell NN interaction. While for total isospin $T = 1$ states rather reliable phase shift analyses exist up to 3 GeV incident energy, for $T = 0$ states the reliability is limited to 1.3 GeV [22, 23]. This situation imposes a severe limit in all existing models of production of mesons heavier than the η meson in pn collisions.

There are basically three different approaches in literature in modeling the production current J based on meson exchange models. One is a microscopic model of $MN \rightarrow M'N'$ reactions whose data are reproduced by the model [3, 11]. The off-shell behavior of the MN T -matrices that are required in the construction of J is then provided by the model. Another approach is a “pseudo” empirical model in which the production current is constructed using the on-shell amplitudes of the $MN \rightarrow M'N'$ as well as $\gamma N \rightarrow M'N'$ reactions extracted directly from the available data [4, 10]. In the latter reaction the VMD is used to convert its on-shell amplitude to an $MN \rightarrow M'N'$ amplitude ($M = \rho, \omega$). The off-shell behavior of the corresponding amplitudes necessary to construct J is then an assumption in this approach. The third approach is to split the MN T -matrix into the pole (T^P) and non-pole (T^{NP}) parts and consider the non-pole part in the Born approximation only in order to construct the production current J [6, 7]. As has been shown elsewhere [25], the MN T -matrix can be split into the pole and non-pole parts according to

$$T = T^P + T^{NP} , \quad (11)$$

where

$$T^P = \sum_B f_{MNB}^\dagger g_B f_{MNB} , \quad (12)$$

with f_{MNB} and g_B denoting the physical meson-nucleon-baryon (MNB) vertex and baryon propagator, respectively. The summation runs over the relevant baryons B . The non-pole part of the T -matrix is given by

$$T^{NP} = V^{NP} + V^{NP}GT^{NP}, \quad (13)$$

where $V^{NP} \equiv V - V^P$, with V^P denoting the pole part of the MN potential V . V^P is given by the equation analogous to Eq.(12) with the renormalized vertices and propagators replaced by the corresponding bare vertices and propagators. This third approach then leads to a production current which is obtained by approximating the full MN T -matrix as $T \cong T^P + V^{NP}$.

3. Our Model

In our model of $NN \rightarrow NNM$, the reaction amplitude M is calculated using Eq.(3). It is based on a relativistic meson exchange model of hadronic interactions. The results we shall show in the next section are obtained by using the NN interaction developed by the Bonn group [18]. This interaction is obtained by solving a three dimensionally reduced (Blankenbecler-Sugar) version of the Bethe-Salpeter equation. The loop integrals in Eq.(3) are calculated consistently with the three dimensional reduction used in constructing the NN interaction, i.e., the two-nucleon propagators $G_{(i,f)}$ are taken to be the Blankenbecler-Sugar propagator. The production current J is modeled according to the third approach discussed in the previous section. It consists of the nucleonic, resonance and mesonic currents as displayed diagrammatically in Fig. 2. Note that they are all Feynman diagrams and, as such, they include both the positive- and negative-energy propagation of the intermediate particles.

All the parameters of our model for the production current (coupling constants and form factors) are confined to the hadronic vertices Γ_{MNB} , $\bar{\Gamma}_{MNB}$ and Γ_{MMM} indicated in Fig. 2 ($B = N, N^*$). Below, we discuss briefly these parameters for each vertex. For more details, see Refs.[7, 8].

$\bar{\Gamma}_{MNB}$: At the meson production vertex $\bar{\Gamma}_{MNN}$, the coupling constant is taken consistently with that used in the construction of the NN interaction. In addition, this vertex contains an extra form factor ($F_N(p^2)$) to account for the off-shellness of the intermediate nucleon, which is far off-shell if a heavy meson is produced. It is given by

$$F_N(p^2) = \frac{\Lambda_N^4}{\Lambda_N^4 + (p^2 - m_N^2)^2}, \quad (14)$$

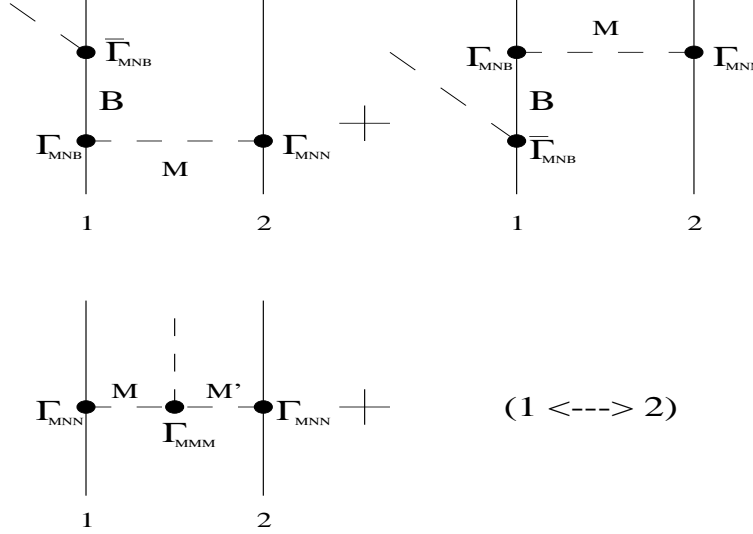


Fig. 2. Model for the meson production current J . The upper two diagrams are called nucleonic or resonance current depending on the intermediate baryon B being a nucleon (N) or a nucleon resonance (N^*). The lower diagram is the mesonic current. $M, M' = \pi, \eta, \rho, \omega, \sigma, a_0$.

with $\Lambda_N = 1.2 \text{ GeV}$. p and m_N stand for the four-momentum and mass of the intermediate nucleon, respectively.

The coupling constant in the vertex $\bar{\Gamma}_{MNN^*}$ is extracted from the measured decay width of the resonance into a meson and a nucleon, $N^* \rightarrow M + N$, whenever available [26]. For the vertex involving a vector meson, the coupling constant can be extracted from the measured radiative decay using the VMD. The sign of the coupling constant is chosen in accordance with the relevant photo-production reaction analysis [27, 28]. $\bar{\Gamma}_{MNN^*}$ is also multiplied by the form factor given by Eq.(14), with m_N replaced by m_{N^*} .

Γ_{MNB} : The vertex Γ_{MNN} is taken consistently with that used in the construction of the NN interaction. For Γ_{MNN} involving the off-shell nucleon that produces the meson, it is also multiplied by the form factor $F_N(p^2)$ given by Eq.(14). The vertex Γ_{MNN^*} is the same as $\bar{\Gamma}_{MNN^*}$, except that it contains an extra form factor due to the off-shell meson which is taken to be the same as that of the corresponding vertex Γ_{MNN} .

Γ_{MMM} : The coupling constants in the three-meson vertices (Γ_{MMM}) are ex-

tracted from both the strong and radiative (measured) decay widths [26] in combination with SU(3) symmetry, plus the OZI rule [29]. The latter relates the basic SU(3) octet and singlet coupling constants. Γ_{MMM} includes the form factor

$$F_M(q^2, q'^2) = \left(\frac{\Lambda_M^2 - m_M^2}{\Lambda_M^2 - q^2} \right) \left(\frac{\Lambda_{M'}^2 - x m_{M'}^2}{\Lambda_{M'}^2 - q'^2} \right), \quad (15)$$

with $\Lambda_M = \Lambda_{M'} = 1.45 \text{ GeV}$. q and q' denote the four momenta of the two mesons with masses m_M and $m_{M'}$, respectively, that fuse to produce the third meson. The parameter $x (= 0, 1)$ ensures the proper normalization according to the normalization point $q'^2 = 0, m_{M'}^2$ at which the corresponding coupling constant is extracted.

There is a number of features in the model described above which are perhaps worth mentioning here. This model is suited for a systematic analysis of the production of different mesons within the same model due to the simplicity of modeling the production current. Also, the model is especially suited for studying the role of different reaction mechanisms that produce a meson. The consistency between the NN interaction and the production current can be easily maintained when one knows the underlying meson exchange structure of the NN interaction used (note that the way the parameters of our model are fixed ensures the consistency between the NN interaction and the production current). As mentioned before, this is critical if one wishes to achieve quantitative predictions, especially for production of heavy mesons.

4. Some selected results

In this section we shall present some selected results on the vector and pseudoscalar meson productions based on the model described in the previous section. As an example of vector meson production, we consider ϕ meson production in pp collisions. For the pseudoscalar meson production, we discuss the results for η production in both the pp and pn collisions.

4.1. $pp \rightarrow pp\phi$

The study of this reaction is of particular importance in connection with the questions related to the amount of hidden strangeness in the

nucleon[30, 31]. In the context of ϕ meson production processes one expects [31] that a large amount of hidden strangeness in the nucleon would manifest itself in reaction cross sections that significantly exceed the values estimated from the OZI rule [29]. This phenomenological rule states that reactions involving disconnected quark lines are forbidden. In the naive quark model the nucleon has no $\bar{s}s$ content, whereas the ϕ meson is an ideally mixed pure $\bar{s}s$ state. Thus, in this case, the OZI rule implies vanishing ϕNN coupling and, accordingly, a negligibly small production of ϕ mesons from nucleons by non-strange hadronic probes. In practice there is a slight deviation from ideal mixing of the vector mesons, which means that the ϕ meson has a small $\bar{u}u + \bar{d}d$ component. Thus, even if the OZI rule is strictly enforced, there is a non-zero coupling of the ϕ to the nucleon, although the coupling is very small. Its value can be used to calculate lower limits for corresponding cross sections. For example, under kinematic conditions chosen to cancel out phase space effects, one expects cross section ratios of reactions involving the production of a ϕ - and an ω meson, respectively, to be

$$R = \frac{\sigma(A + B \rightarrow \phi X)}{\sigma(A + B \rightarrow \omega X)} \approx \tan^2(\alpha_V) , \quad (16)$$

where A, B and X are systems that do not contain strange quarks. $\alpha_V \equiv \theta_V - \theta_{V(ideal)}$ is the deviation from the ideal $\omega - \phi$ mixing angle. This result arises from simply equating the cross section ratio to the square of the ratio of the relevant coupling constants at the ϕ and ω production vertices. According to the OZI rule plus SU(3) symmetry, these couplings are proportional to $\sin(\alpha_V)$ and $\cos(\alpha_V)$, respectively. With the value $\alpha_V \cong 3.7^\circ$ [26] one gets a rather small ratio of $R = 4.2 \times 10^{-3}$. The data presented by the DISTO collaboration [32, 33] in pp collisions indicate that this ratio, after correcting for phase space effects, is about eight times larger than the above OZI estimate.

In principle, the ϕ meson production cross section can be used for a direct determination of the ϕNN coupling strength. Any appreciable ϕNN coupling in excess of the value given by the OZI rule ($g_{\phi NN} \cong -(0.60 \pm 0.15)$) [7] could be interpreted as evidence for hidden strangeness in the nucleon. Of course, there is also an alternative picture: one in which the coupling of the ϕ meson to the nucleon does not occur via possible $\bar{s}s$ components in the nucleon, but via intermediate states with strangeness. Specifically, this means that the ϕ meson couples to the nucleon via virtual $\Lambda K, \Sigma K$, etc. states. Corresponding model calculations [34, 35] have shown, however, that such processes give rise to (effective) ϕNN coupling constants comparable to the OZI values and therefore should not play a role in drawing conclusions concerning hidden strangeness in the nucleon.

Details of our calculation may be found in Ref.[7]. The work of Ref.[7] is a combined analysis of the ω and ϕ meson production in pp collisions in order to reduce the number of free parameters in the model. Here we only report on the essential results. For the production current J we consider only the nucleonic and mesonic currents. The latter consists of $\nu\rho\pi$ exchange current ($\nu = \omega, \phi$). Other mesonic currents have been investigated in a systematic way and found to be very small. The nucleon resonance current is not considered because, presently, there is no established resonance that decays into a vector meson and a nucleon (see Ref.[36] in this connection). It is found that the ϕ meson is produced significantly from the $\phi\rho\pi$ exchange current in pp collisions. This means that one must be able to disentangle this current from the nucleonic current (where the ϕ meson is emitted directly from the nucleon) if one wishes to extract the ϕNN coupling strength from this reaction. As pointed out in Ref.[5], this can be done by looking at the angular distribution of the emitted meson. Because the mesonic current contribution yields an isotropic angular distribution, whereas the nucleonic current contribution exhibits a $\cos^2(\theta)$ dependence, the two currents can be disentangled uniquely from the angular distribution data. Fig. 3 illustrates this point for the $pp \rightarrow pp\omega$ reaction at a proton beam energy of 2.2 GeV . The upper panel illustrates the situation when the nucleonic current (dashed curve) is smaller than the mesonic current (dash-dotted curve) resulting in a nearly flat angular distribution (solid curve). Note that the interference between the two currents is destructive, which is a direct consequence of the signs of the relevant coupling constants determined in our model as discussed in the previous section. The lower panel shows the situation when the nucleonic current is larger than the mesonic current. Here the angular distribution exhibits a pronounced angular dependence. In both scenarios the total cross sections have been kept to be about the same.

The earlier data of the ϕ meson angular distribution by the DISTO collaboration [32] at a proton beam energy of 2.85 GeV is shown in Fig. 4 together with our result. The absolute normalization of this data has been determined as described in Ref.[7]. Although the data have large uncertainties, the observed angular distribution is rather flat. Note that the angular distribution should be symmetric about $\theta = 90^\circ$, due to the identity of the two protons. The solid curve is one of our calculations fitted to the data. The dash-dotted and dashed curves are the corresponding mesonic and nucleonic current contributions, respectively. As one can see, the data require a very small contribution from the nucleonic current. The value of the ϕNN coupling constant thus extracted is in the range $g_{\phi NN} \approx -(0.2 - 0.9)$. More data for both the ϕ and ω meson at low excess energies are necessary in order to determine better the parameters of the model, and thus reduce the uncertainties in the extracted value of $g_{\phi NN}$. In this connection, current ex-

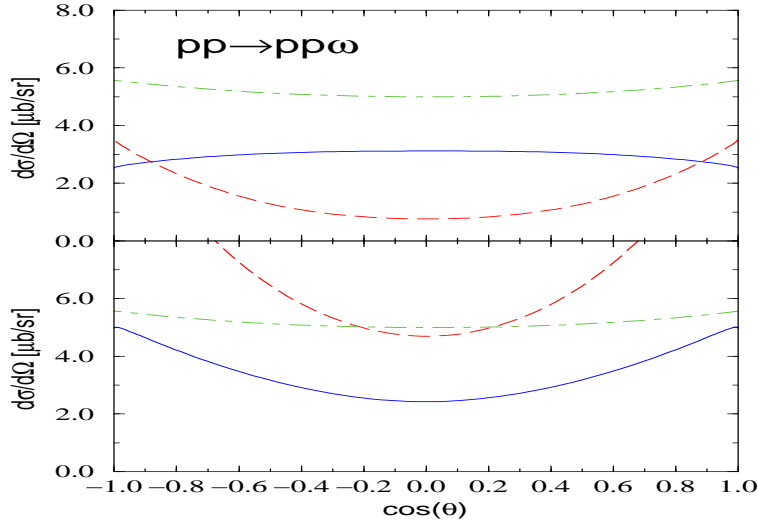


Fig. 3. Angular distribution of the emitted ω meson in the c.m. frame of the total system for two possible scenarios at a proton incident energy of 2.2 GeV. The upper panel corresponds to the case when the nucleonic current is smaller than the mesonic current. The lower panel corresponds to the case when the nucleonic current is larger than the mesonic current. The dashed curves represent the nucleonic current contribution while the dash-dotted curves represent the mesonic current contribution. The solid curves correspond to the total contribution.

perimental efforts at COSY (see contributions by M. Wolke, D. Grzonka and A. Khoukaz at this meeting) are of particular interest. In any case, the value extracted here is compatible with the OZI value of $g_{\phi NN} \cong -(0.60 \pm 0.15)$. More recent data with an improved data analysis from the DISTO collaboration [33] exhibit a nearly isotropic angular distribution, corroborating a very small nucleonic current contribution.

Fig. 5 shows the predicted total cross section ratio $R_{\phi/\omega} = \sigma_{pp \rightarrow pp\phi} / \sigma_{pp \rightarrow pp\omega}$ as a function of excess energy. For low excess energies, the predicted ratio is about 4 to 7 times that of the OZI estimate. At higher energies, the enhancement over the OZI estimate decreases to a factor of 3 or so. What then is the origin of this enhancement over the OZI estimate as predicted by our model? One source of the enhancement is in the mesonic current. As discussed in detail in Ref. [7], the violation of the OZI rule at the $\phi\rho\pi$ vertex had to be introduced in order to achieve a simultaneous and consistent description of the then available data on the reactions $pp \rightarrow pp\omega$ and $pp \rightarrow pp\phi$. This explicit OZI violation in terms of the $\phi\rho\pi$ and $\omega\rho\pi$ coupling constants used suggests an enhancement of around 3 in the cross

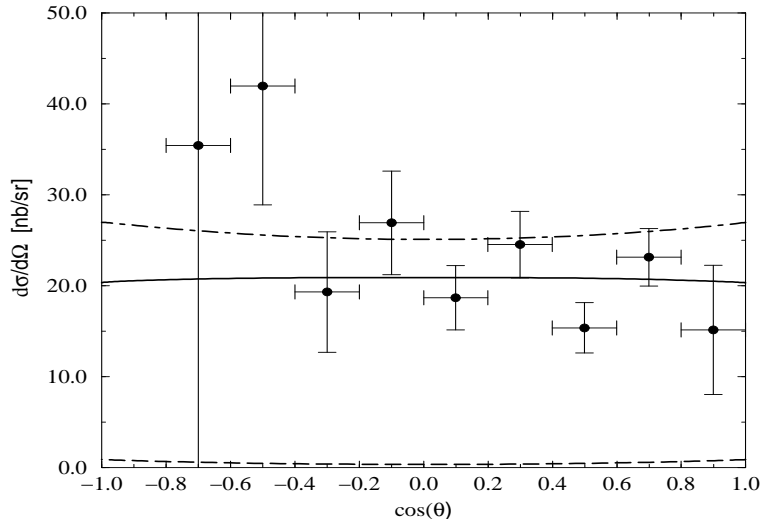


Fig. 4. Angular distribution of the emitted ϕ meson in the c.m. frame of the total system at a proton incident energy of 2.85 GeV. The dashed curve corresponds to the nucleonic current contribution while the dash-dotted curve to the mesonic current contribution. The solid curve corresponds to the total contribution. The data are from Ref.[32]. The absolute normalization of the data has been determined as described in Ref.[7].

section ratio. With regard to the nucleonic current, the employed ωNN and ϕNN coupling constants lead to results that exceed the OZI value only in one case: namely for the parameter set with $g_{\phi NN} = -0.9$ [7]. The corresponding enhancement factor for the cross section ratio amounts to about 2. It is then evident from the above consideration that the cross section ratios resulting from the model calculation differ significantly from those values implied by the employed coupling constants. Obviously, dynamical effects such as interferences, etc., play a rather important role here and can lead to a fairly large deviations from the OZI prediction within a conventional picture, i.e., without introducing any “exotic” mechanisms. Consequently, one should be very cautious in drawing direct conclusions regarding the strangeness content in the nucleon from such cross section ratios. The behavior of the cross section ratio as the excess energy approaches zero is due to the finite width of the ω , which prevents the ω meson production cross section from decreasing rapidly, as it does in the case of ϕ meson.

Evidently, the enhancement of a factor of 3 or so over the OZI estimate at higher excess energies in Fig. 5 is much smaller than the enhancement over the OZI prediction of about a factor 10 found by the DISTO collaboration

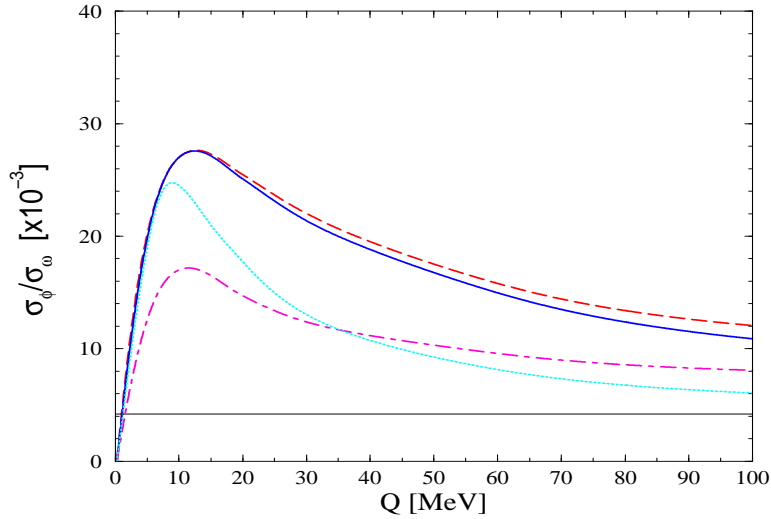


Fig. 5. Total cross section ratio $R_{\phi/\omega} = \sigma_{pp \rightarrow pp\phi} / \sigma_{pp \rightarrow pp\omega}$ as a function of excess energy. Different curves correspond to the possible sets of parameters as determined in Ref.[7]. The horizontal line corresponds to the OZI prediction.

[32] at an excess energy $Q \approx 80$ MeV in ϕ meson production. However, it is important to realize that their measurement was done at a fixed incident beam energy of 2.85 GeV, and therefore the corresponding excess energy of the produced ω is already 319 MeV. Though corrections for the differences in the available phase space were obviously applied when extracting the above result, there are other effects that may influence the ratio, such as the energy dependence of the production amplitude, the onset of higher partial waves, etc., that cannot be corrected for easily. It is therefore possible that the actual deviation in the value of $R_{\phi/\omega}$ from the OZI prediction is also smaller. Thus, it would be interesting to perform a measurement of the cross section ratio at the same (or at least similar) excess energies. From the theoretical side, the newer data on ϕ production by the DISTO collaboration [33] and, especially, the new data on ω production from COSY, which will become available soon [37] (see also the contribution by A. Khoukaz at this meeting), should already impose much more stringent constraints on the parameters of our model and help address better the problem of OZI violation and related issues in NN collisions. In fact, these new data seem to indicate that we overpredict the ω meson production cross section above $Q \sim 30$ MeV. This has a direct implication on the cross section ratio $R_{\phi/\omega}$ at higher excess energies as discussed above.

4.2. $NN \rightarrow NN\eta$

We now turn to the production of pseudoscalar mesons. Here we confine our discussion to the production of η meson in NN collisions. The production of this meson near the threshold energy is of special interest, since the existing data are by far the most accurate and complete among those for heavy meson production and, consequently, they offer a possibility to investigate this reaction in much more detail than any of the other heavy meson production reactions. In addition to the total cross sections for the $pp \rightarrow pp\eta$ reaction [38, 39, 40, 41, 42], we have data for $pn \rightarrow pn\eta$ [43] and $pn \rightarrow d\eta$ [42, 44]. The differential cross section data for the $pp \rightarrow pp\eta$ reaction [45] are available as well. Consequently, there is a large number of theoretical investigations on these reactions. The production of η mesons in NN collisions is thought to occur predominantly through the excitation (and de-excitation) of the $S_{11}(1535)$ resonance, to which the η meson couples strongly. However, the excitation mechanism of this resonance is currently an open issue. For example, Batinić et al. [3] (see also the contribution by S. Ceci to this meeting) have found both the π and η exchange as the dominant excitation mechanism. However, they have considered only the $pp \rightarrow pp\eta$ reaction. Gedalin et al. [6] and Fäldt and Wilkin [10] have considered both the $pp \rightarrow pp\eta$ and $pn \rightarrow pn\eta$ reactions. In the analysis of Ref.[10] the $pn \rightarrow d\eta$ reaction was also included. These authors [6, 10] find the ρ exchange to be the dominant excitation mechanism of the $S_{11}(1535)$ resonance. In particular, it has been claimed [10] that ρ meson exchange is important for explaining the observed shape of the angular distribution in the $pp \rightarrow pp\eta$ reaction. We also mention that, in contrast to the dominant resonance current contribution found in Refs.[3, 6, 10], in a recent calculation of the $pp \rightarrow pp\eta$ reaction by Peña et al. [9], it is found that the dominant contribution arises not from the $S_{11}(1535)$ resonance current, but from what they refer to as the short range amplitude. In our language this corresponds to the shorter range part of the nucleonic current. Here we shall report on yet another possible scenario that reproduces both the $pp \rightarrow pp\eta$ and $pn \rightarrow pn\eta$ reactions and discuss a possibility to disentangle these reaction mechanisms.

Although here we shall confine ourselves to the problem just mentioned, the description of η meson production in NN collisions presents other interesting aspects. For example, the η meson interacts much more strongly with the nucleon than do mesons like the pion so that not only the NN FSI, but also the ηN FSI is likely to play an important role, thereby offering an excellent opportunity to learn about the ηN interaction at low energies. In fact, the near-threshold energy dependence of the observed total cross section for η meson production differs from that of pion and η' production, which follow

the energy dependence given simply by the available phase-space together with the NN FSI. The enhancement of the measured cross section at small excess energies in η production compared to those in π and η' production is generally attributed to the strong attractive ηN FSI. In addition to all these issues, the theoretical understanding of η meson production in NN collisions near threshold in free space is also required for investigating the dynamics of the $S_{11}(1535)$ resonance in the nuclear medium, possible existence of ηNN bound states, and the possibility of using η to reveal the properties of high-density nuclear matter created in relativistic heavy-ion collisions.

Our model for the η production current includes the nucleonic, mesonic and resonance currents. The mesonic current consists of the $\eta\rho\rho$, $\eta\omega\omega$, and $\eta a_0\pi$ exchange contributions. The resonance current consists of the $S_{11}(1535)$, $P_{11}(1440)$, and $D_{13}(1520)$ resonances excited via π , η , ρ and ω exchange. For the NN FSI, we use the Bonn interaction [18]. For the NN ISI, we consider only the on-shell interaction obtained from Ref.[22]. The details of the calculation will be reported elsewhere [46]. The results for the total cross section as a function of excess energy are shown in Fig. 6. The

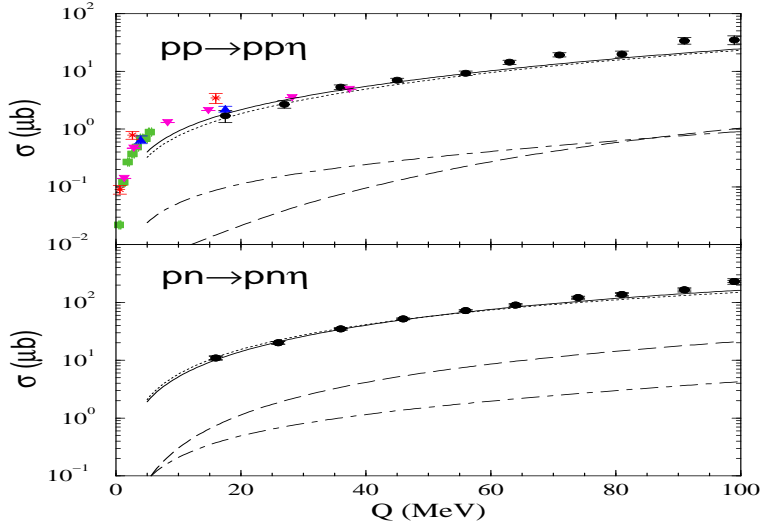


Fig. 6. Total cross sections for the $pp \rightarrow pp\eta$ (upper panel) and $pn \rightarrow pn\eta$ (lower panel) reactions as a function of excess energy. The dashed curves correspond to the nucleonic current contribution while the dash-dotted curves to the mesonic current contribution; the dotted curves represent the resonance current contribution. The solid curves are the total contribution. The data are from Refs.[38, 39, 40, 41, 42, 43].

upper panel shows the results for pp collisions while the lower panel those for pn collisions. The dashed curves are the nucleonic current contribution; the dash-dotted curves correspond to the mesonic current and the dotted curves to the resonance current. The solid curves are the total contribution. As one can see, the total cross sections are dominated by the resonance current, and more specifically by the strong $S_{11}(1535)$ resonance (see Fig. 7). Our nucleonic current contributions (dashed curves) are much smaller than the resonance current contributions. This is in contradiction to the findings of Ref.[9]; there, instead of the resonance current, the short range amplitude (shorter range part of the nucleonic current) gives a large contribution to the $pp \rightarrow pp\eta$ cross section. For small excess energies, our calculation underpredicts the data. As mentioned above, this is usually attributed to the ηN FSI, which is not accounted for in the present model. Note that the results for $pn \rightarrow pn\eta$ with excess energy $Q > 50 \text{ MeV}$, corresponding to incident beam energy larger than 1.3 GeV , should be interpreted with caution, as no reliable NN phase shift analyses for $T = 0$ states exist at present for energies above 1.3 GeV [23].

In Fig. 7 the $S_{11}(1535)$ resonance contribution to the total cross sections is shown (solid curves), together with the contribution from the individual meson exchange excitation mechanism. The dashed curves correspond to the π exchange, while the dash-dotted curves correspond to the η exchange contribution. The dotted curve is due to ρ exchange. Although the ω exchange is included in the calculation, its contribution is not shown here separately because it is much smaller than the ρ exchange contribution. As can be seen, the dominant contribution is due to the π exchange followed by η exchange. The ρ exchange is very small. Several observations are in order here:

- 1) The major reason for the small ρ exchange contribution, in contrast to the result of Refs.[6, 10], is that in our model we have not allowed the vector (γ^μ) coupling in the ρNN^* vertex for spin-1/2 resonances. Note that for an odd-parity spin-1/2 resonance, there is an overall extra γ^5 factor. Unlike the case of ρNN vertex, the presence of this coupling in the ρNN^* vertex leads to a violation of gauge invariance, which is especially relevant when used in connection with the VMD. As mentioned in the previous section, the ρNN^* coupling constant in our model is extracted from the radiative decay, $N^* \rightarrow \gamma + N$, using the VMD. The simplest way of satisfying the gauge invariance constraint is to omit the γ^μ coupling from the ρNN^* vertex, which we have done in the present work. Note that the tensor ($\sigma^{\mu\nu}$) coupling is free of this problem. A direct consequence of omitting the vector coupling in the ρNN^* vertex is a very small ρ exchange contribution to the cross section as shown in Fig. 7. Note that in Ref.[6] the $\rho NS(1535)$

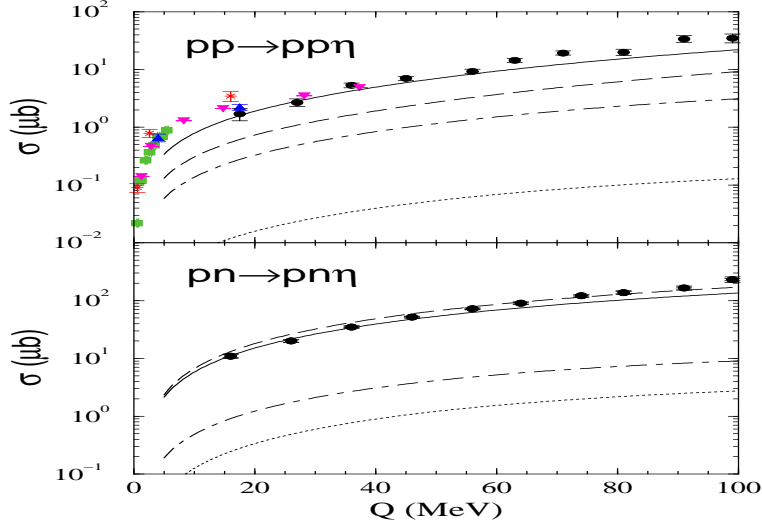


Fig. 7. Same as Fig. 6, except that it shows the $S_{11}(1535)$ resonance contribution only. The dashed curves correspond to the π exchange contribution while the dash-dotted curves to the η exchange contribution; the dotted curves represent the ρ exchange contribution. The solid curves show the total contribution.

vertex is given by the $\gamma^5 \gamma^\mu$ coupling. An alternative to avoid the gauge invariance problem while keeping the γ^μ term is to use a vertex of the form $\Gamma^\pm [\gamma^\mu q^2 - (m_{N^*} \mp m_N) q^\mu]$ [24], where $\Gamma^- \equiv \gamma^5$ and $\Gamma^+ \equiv 1$. In fact, Peña et al. [9] have used a modified version of this vertex in conjunction with the coupling constant determined from a quark model [24]. They found a non-negligible contribution of the ρ exchange to the excitation of $S_{11}(1535)$ in $pp \rightarrow pp\eta$. Relevant experimental information should decide whether the vector coupling is required or not in the ρNN^* vertex.

- 2) The η exchange contribution is relatively large in the present calculation. In fact, in the case of $pp \rightarrow pp\eta$ its contribution to the cross section is about half of that due to the π exchange. The ηNN coupling strength is subject to a rather large uncertainty; the value of this coupling constant ranges from $g_{NN\eta} \sim 2.7$ to $g_{NN\eta} \sim 6.4$ [27]. The relatively large contribution of η here result from using the ηNN coupling constant of $g_{\eta NN} = 6.14$, as used in the construction of the Bonn NN interaction [18]. This value is close to the upper limit. However, the η meson exchange in the Bonn potential [18] might just be an exchange of a $(J^P, T) = (0^-, 0)$ quantum number and not of a

genuine η meson. Consequently, the contribution from η exchange is subject to this uncertainty in the coupling constant. Anyway, in the present calculation for $pp \rightarrow pp\eta$, the η exchange interferes constructively with the dominant π exchange contribution, yielding the total contribution as shown by the solid line in Fig. 7. For $pn \rightarrow pn\eta$, the η exchange interferes constructively with the π exchange in the $T = 1$ channel (as in the case of $pp \rightarrow pp\eta$), but destructively in the $T = 0$ channel due to the isospin factor -3 in the π exchange amplitude.

- 3) The correct description of both $pp \rightarrow pp\eta$ and $pn \rightarrow pn\eta$ reactions depends not only on different isospin factors involved for isoscalar and isovector mesons exchanged but, also on a delicate interplay between the NN FSI and ISI in each partial wave involved. While the NN FSI enhances the total cross section, the NN ISI has an opposite effect (see discussion in section II). In this connection, we mention that in Ref.[10] the reduction factor due to the NN ISI is estimated to be about $(0.77)^2 = 0.59$ due to the 3P_0 state and $(0.73)^2 = 0.53$ due to 1P_1 . In our calculation, however, the corresponding reduction factors are about 0.19 and 0.27 near the threshold energy. This large discrepancy between the results of Ref.[10] and ours is due to the fact that, whereas our reduction factor is given by Eq.(10), the reduction factor in Ref.[10] is given by $\lambda \equiv \eta_L^2 = (e^{-Im(\delta_L)})^2$. We argue that the latter formula is inappropriate to estimate the effect of the NN ISI for it does exhibit a pathological feature: namely, when the absorption is maximum ($\eta_L = 0$), this formula yields $\lambda = 0$, implying the total absence of the NN elastic channel and thus not allowing the production reaction to occur. However, scattering theory tells us that when the absorption cross section is maximum, the corresponding elastic cross section does not vanish, but is 1/4 of the absorption cross section. Note that this feature is present in Eq.(10). Furthermore, the authors of Ref.[10] apparently have identified incorrectly the inelasticity η_L with $\cos^2(\rho)$, where ρ is one of the two parameters (the other is the phase shift) given in Ref.[22]. The phase shift parametrization given in Ref.[22] differs from the standard Stapp parametrization as given by Eq.(8). It is obvious that with a more appropriate estimate of the reduction factor λ as given by Eq.(10) the result of Ref.[10] would underpredict considerably the cross section data.

Fig. 8 shows the predicted angular distribution of η in $pp \rightarrow pp\eta$ at an excess energy of $Q = 37$ MeV together with the data of Ref.[45]. Again, the resonance contribution (dotted curve) dominates the cross section. As pointed out in Ref.[10], the shape of the angular distribution of the latter contribution bends upwards at the forward and backward angles due to the π

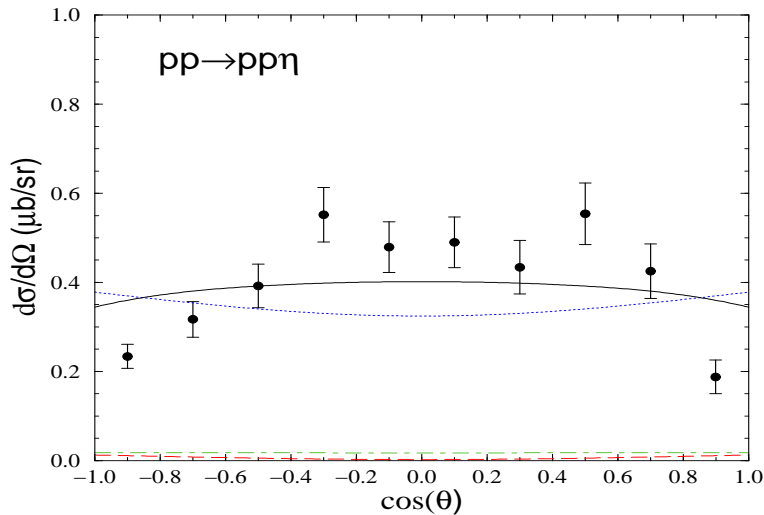


Fig. 8. Angular distribution of the emitted η meson in the c.m. frame of the total system at an excess energy of $Q = 37 \text{ MeV}$. The dashed curve corresponds to the nucleonic current contribution while the dash-dotted curve to the mesonic current contribution; the dotted curves represent the resonance current contribution. The solid curve show the total contribution. The data are from Ref.[45].

exchange dominance in the $S_{11}(1535)$ resonance contribution. However, due to an interference with the nucleonic (dashed) and mesonic (dash-dotted) currents, the shape of the resulting angular distribution (solid curve) is inverted with respect to that of the resonance current contribution alone. As one can see, although the overall magnitude is rather well reproduced, the rather strong angular dependence exhibited by the data is not reproduced by our model. At this point one might argue that the excitation mechanism of the $S_{11}(1535)$ resonance as given by the present model is not correct and that, indeed, the ρ meson exchange should give the dominant contribution, as has been claimed in Ref.[10]. However, judging the level of agreements between the predictions of Ref.[10] and ours with the data, one cannot discard the dominance of π and η exchange in favor of the ρ exchange mechanism for exciting the $S_{11}(1535)$ resonance. In this connection, we mention that the new data from COSY which will become available soon shows a flat angular distribution [47].

From the above considerations, we conclude that, at present, the excitation mechanism of the $S_{11}(1535)$ resonance in NN collisions is still an open question. Indeed, we have just offered a scenario other than the ρ exchange mechanism that reproduces the available data equally well. It is therefore

of special interest to seek a way to disentangle these possible scenarios. In this connection, spin observables may potentially help resolve this issue. According to Ref.[10], the ρ exchange contribution is expected to lead to an analyzing power given by

$$A_y = A_y^{max} \sin(2\theta) \quad (17)$$

in $pp \rightarrow pp\eta$, where A_y^{max} is positive for low excess energies, peaking at $Q \approx 10 \text{ MeV}$ and becoming negative for excess energies $Q > 35 \text{ MeV}$. The results (dashed curves) at $Q = 10 \text{ MeV}$ (upper panel) and $Q = 37 \text{ MeV}$ (lower panel) are shown in Fig. 9. The corresponding predictions of the present model are also shown (solid curves). The different features exhib-

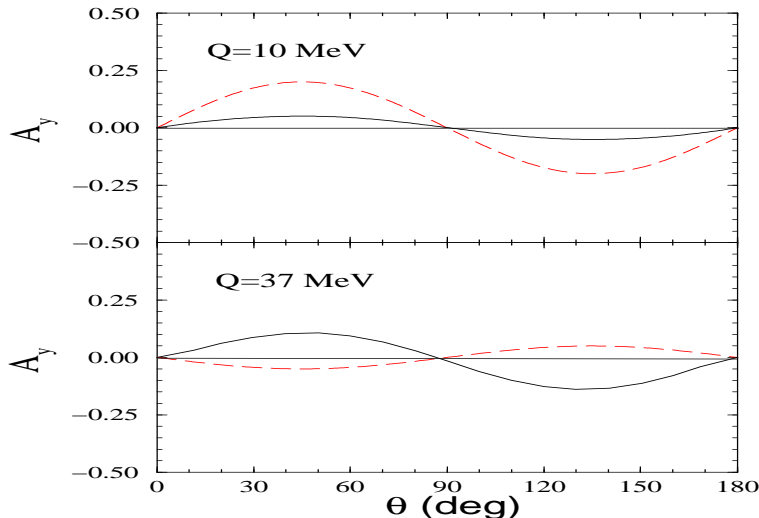


Fig. 9. Analyzing power for the reaction $pp \rightarrow pp\eta$ as a function of emission-angle of η in the c.m. frame of the total system at an excess energy of $Q = 10 \text{ MeV}$ (upper panel) and $Q = 37 \text{ MeV}$ (lower panel). The dashed curve corresponds to the case of ρ exchange dominance according to Ref.[10]. The solid curve corresponds to the present model calculation.

ited by the two scenarios for the excitation mechanism of the $S_{11}(1353)$ is evident. In this connection, the COSY11 effort to measure the analyzing power in $pp \rightarrow pp\eta$ (see the contribution by P. Winter in this meeting) is of great importance. We emphasize that these different results should be interpreted with caution. The reason for this is that, as mentioned before, the present model accounts for the NN ISI only in the on-shell approximation. While this may be a reasonable approximation for calculating cross

sections, it may introduce rather large uncertainties in the calculated spin observables.

5. Summary

The production of heavy mesons in NN collisions has been discussed within the meson exchange model of hadronic interactions, paying special attention to the basic dynamics that determine the behavior of the cross sections near the threshold energy. Differences in the existing meson exchange models as well as their limitations have been also discussed. Heavy meson production processes necessarily probe the short range dynamics, a domain where we have very limited knowledge so far. In this regime even the relevant reaction mechanisms are largely unknown. The theory of heavy meson production in NN collisions is still in its early stage of development. Successful description of these processes in terms of purely hadronic degrees of freedom calls for correlation of as many independent data as possible in a consistent way. The $pp \rightarrow pp\phi$ reaction has been discussed as an example of the production of vector mesons in NN collisions. As for the pseudoscalar meson production, results for the η production in both the pp and pn collisions were presented. From these examples, it is clear that not only the $pp \rightarrow ppM$, but also the $pn \rightarrow pnM$ and $pn \rightarrow dM$ reactions should be investigated. Also more exclusive observables than the total cross section such as the spin observables should be studied.

Acknowledgment I would like to take this opportunity to thank the organizers of this symposium for inviting me to present this lecture. I also thank H. Arellano, J. Durso, J. Haidenbauer, C. Hanhart, H. Lee, J. Speth, and A. Szczurek who have collaborated in our study of heavy meson production reactions at one stage or another. I thank J. Durso, J. Haidenbauer and C. Hanhart for a careful reading of this manuscript.

REFERENCES

- [1] C.Hanhart, U. van Kolck and G. A. Miller, Phys. Rev. Lett. **85**, 2905 (2000), and references therein.
- [2] M. P. Rekalo, J. Arvieux and E. Tomasi-Gustafsson, Phys. Rev. **C55**, 2630 (1997); A. B. Santra and B. K. Jain, Nucl. Phys. **A634**, 309 (1998); E. Gedalin, A. Moalem and L. Razdolskaja, Nucl. Phys. **A650**, 471 (1999); K. Nakayama, J. Haidenbauer and J. Speth, Phys. Rev. **C63**, 015201 (2000); A. I. Titov, B. Kämpfer and B. L. Reznik, Eur. Phys. J. **A7**, 543 (2000); V. Yu. Grishina et al., Phys. Lett. **B475**, 9 (2000).
- [3] M. Batinić, A. Svarc and T.-S. H. Lee, *Phys.Scripta* **56**, 321 (1997).
- [4] A. Sibirtsev and W. Cassing, Eur. Phys. J. **A2**, 333 (1998).
- [5] K. Nakayama et al., Phys. Rev. **C57**, 1580 (1998).
- [6] E. Gedalin, A. Moalem and L. Razdolskaja, Nucl. Phys. **A634**, 368 (1998).
- [7] K. Nakayama et al., Phys. Rev. **C60**, 055209 (1999).
- [8] K. Nakayama et al., Phys. Rev. **C61**, 024001 (1999).
- [9] M. T. Peña, H. Garcilazo and D. O. Riska, Nucl. Phys. **A683**, 322 (2001).
- [10] G. Fäldt and C. Wilkin, nucl-th/0104081.
- [11] V. Baru et al., in preparation.
- [12] V. Bernard, N. Kaiser and U. Meißner, Eur. Phys. J. **A4**, 259 (1999); N. Kaiser, Phys. Rev. **C60**, 057001(1999);
- [13] S. Ahlig et al., Phys. Rev. **D64**, 014004 (2001).
- [14] S. Wycech and A. M. Green, Nucl. Phys. **663&664**, 529c (2000); A. Fix and H. Arenhövel, nucl-th/0104032 and references therein.
- [15] F. E. Low, Phys. Rev. **110**, 974 (1958).
- [16] K. Watson, Phys. Rev. **88**, 1163 (1952). For a recent discussion, see Ref.[21].
- [17] A. Moalem, L. Razdolskaja and E. Gedalin, hep-ph/9505264.
- [18] R. Machleidt, Adv. Nucl. Phys. **19**, 189 (1989).
- [19] M. Lacombe, B. Loiseau, J. M. Richard, R. Vinh Mau, J. Côté, P. Pirès and R. de Tourreil, Phys. Rev. **C21**, 861 (1980).
- [20] T. Rijken and V. G. J. Stoks, Phys. Rev. **C59**, 21 (1999).
- [21] C. Hanhart and K. Nakayama, Phys. Lett. **B454**, 176 (1999).
- [22] extracted from the VIRGINIA TECH PARTIAL-WAVE ANALYSES ONLINE (http://said.phys.vt.edu/said_branch.html)
- [23] I. Strakovsky, private communication.
- [24] D. O. Riska and G. E. Brown, Nucl. Phys. **A679**, 577 (2001).
- [25] B. C. Pearce and I. R. Afnan, Phys. Rev. **C34**, 991 (1986).
- [26] Particle Data Group, Eur. Phys. J. **C3**, 1 (1998).

- [27] M. Benmerrouche and N. C. Mukhopadhyay, Phys. Rev. **D51**, 3237 (1995).
- [28] J. F. Zhang, N. Mukhopadhyay and M. Benmerrouche, Phys. Rev. **C52**, 1134 (1995); H. Garcilazo and E. Moya de Guerra, Nucl. Phys. **A562**, 521 (1993); A. Yu. Korchin, O. Scholten and R. G. E. Timmermans, Phys. Lett. **B438**, 1 (1998).
- [29] S. Okubo, Phys. Lett. **5**, 165 (1963); G. Zweig, CERN Report No. TH412, 1964; J. Iizuka, Prog. Theor. Phys. Suppl. **37 & 38**, 21 (1966).
- [30] J.F. Donoghue and C.R. Nappi, Phys. Lett. **B168**, 105 (1986); J. Gasser, H. Leutwyler and M.E. Sainio, Phys. Lett. **B253**, 252 (1991); J. Ashman et al., Phys. Lett. **B206**, 364 (1988).
- [31] J. Ellis, E. Gabathuler and M. Karliner, Phys. Lett. **B217**, 173 (1989); E.M. Henley, G. Krein and A.G. Williams, Phys. Lett. **B281**, 178 (1992).
- [32] F. Balestra et al., Phys. Rev. Lett. **81**, 4572 (1998).
- [33] F. Balestra et al., Phys. Rev. **C63**, 024004 (2001).
- [34] P. Geiger and N. Isgur, Phys. Rev. **D55**, 299 (1997).
- [35] Ulf-G. Meißner, V. Mull, J. Speth and J.W. Van Orden, Phys. Lett. **B408**, 381 (1997).
- [36] S. Capstick and W. Roberts, Phys. Rev. **D49**, 4570 (1994); Q. Zhao, H. Li and C. Bennhold, Phys. Lett. **B436**, 42 (1998); *ibid* Phys. Rev. **C58**, 2393 (1998); Y. Oh, A. Titov and T.-S. H. Lee, nucl-th/0104046;
- [37] K. Birkman, private communication; S. A. El-Samad et al., nucl-ex/0107009.
- [38] E. Chiavassa et al., Phys. Lett. **B322**, 270 (1994).
- [39] F. Hibou et al., Phys. Lett. **B438**, 41 (1998).
- [40] H. Calén et al., Phys. Lett. **B366**, 39 (1996).
- [41] J. Smyrski et al., Phys. Lett. **B474**, 182 (2000).
- [42] H. Calén et al., Phys. Rev. Lett. **79**, 2642 (1997).
- [43] H. Calén et al., Phys. Rev. **C58**, 2667 (1998).
- [44] H. Calén et al., Phys. Rev. Lett. **80**, 2069 (1998).
- [45] H. Calén et al., Phys. Lett. **B458**, 190 (1999).
- [46] K. Nakayama, T.-S. H. Lee and J. Speth, in preparation
- [47] K. Kilian, private communication.